Hindawi
Journal of Electrical and Computer Engineering
Volume 2022, Article ID 7071316, 9 pages
https://doi.org/10.1155/2022/7071316

Research Article

A New Adaptive Switching Control Method for the Complex Operating Condition of the Grid-Connected Power System

Miao Yu,[1,2,3] **Yihui Zhang**,[1,2] **Shouzhi Zhang**,[1,2] **Jingxuan Hu**,[1,2] **Shuwei Yang**,[1,2] **Weijie Du**,[1,2] **and Jinglin Li**[1,2]

[1]*School of Mechanical-Electronic and Automobile Engineering, Beijing University of Civil Engineering and Architecture, Beijing 100044, China*
[2]*Beijing Key Laboratory of Service Performance of Urban Rail Transit Vehicles, Beijing University of Civil Engineering and Architecture, Beijing 100044, China*
[3]*State Key Laboratory of Control and Simulation of Power System and Generation Equipment, Tsinghua University, Beijing 100084, China*

Correspondence should be addressed to Miao Yu; olivermiaoer@163.com

Received 13 July 2022; Revised 1 October 2022; Accepted 25 October 2022; Published 28 October 2022

Academic Editor: Rossano Musca

Due to the increase in wind power accessing power system in recent years, the low-frequency oscillation of power system is more complicated. Therefore, a new adaptive switching control method combined with a nonlinear system is proposed for the complex operating conditions of the grid-connected power system. Firstly, this method decomposes the low-frequency oscillation control problem of the power system into two parts, which are the linear system control and the nonlinear system control. Then, in the linear system control part, the iterative identification method is used to control this part. In the nonlinear system control part, the nonlinear term is decomposed into a combination of the previous beating measurable and the nonlinear estimation increment. Secondly, the nonlinear system is divided into three different operating conditions by the nonlinear estimation increment. Thus, four different adaptive controllers are obtained. Then, the designed controller is switched according to the controlled object with four controllers by the switching function, which not only ensures the stability of the closed-loop system, but also improves the control performance of the controller under different operating conditions. Finally, the feasibility and effectiveness of this method are verified, and the controller can fit the control efficiency of the real power system well.

1. Introduction

In recent years, with the colossal increasing in the scale of the power system, the uncertainty and complexity have been exacerbated. However, wind farms in China are characterized by the large-scale, high and long-distance transmission, and the connection between regional power grids with a high proportion of wind power penetration is even weaker. Especially on transmission lines with long distance and heavy load, the operation characteristics and load control modes of wind farms are different, which increases the difficulty of analysis and control of wind power integration. The question of how to ensure the stability of the power system is still a difficult problem faced by power researchers.

Wind energy, as a renewable clean energy, is widely used and its large-scale access will have a certain impact on the safe and stable operation of the power grid, which may increase the risk of low-frequency oscillation in the power system. Therefore, the research on the control method of low-frequency oscillation generated by the large-scale wind power connected to the system has become a hot topic focused by many scholars.

In theoretical research field on low-frequency oscillations, [1] used the combination of the EWT and Prony algorithm. The noise in the PMU acquisition signal was filtered by EWT decomposition and reconstruction, and the derivative method was introduced to improve the real order while maintaining the fitting accuracy. [2] clarified the

mechanism of the excitation system that influenced the frequency oscillation and the PSS analysis method that influenced the frequency oscillation damping and presented the evaluation method of different PSS generators that influenced the frequency oscillation mode. [3] proposed an analysis of the low-frequency oscillation based on the vector margin method. This method could calculate the influence of multiple DFIGs on the low-frequency oscillation mode of the system when they were connected to the power grid at the same time and made the analysis results clearer and more intuitive by the method of two-dimensional complex plane diagram. However, when the operating mode of the system changed, the influence of each wind turbine on the stability of the system could not change with the change of the operating mode.

Regarding the low-frequency oscillation control method, [4] used a coordinated control method of ADRC and the traditional wide-area power system stabilizer (PSS), which could suppress the low-frequency oscillation of the system more effectively through the compensation for disturbance estimation, and had strong adaptability and robustness. [5] proposed a coordinated optimization method of PSS parameters in multiple operation modes based on a moth-to-fire optimization algorithm. This method could effectively improve the dynamic stability of the system, had good adaptability to various operation modes, and the algorithm itself had strong convergence. [6] presented a method for selecting PSS to be optimized considering both low-frequency oscillations and frequency oscillations in multimachine systems. This method could effectively suppress the frequency oscillation and significantly increase the damping ratio of the frequency oscillation, thus suppressing the frequency oscillation. [7] proposed a parameter design method for PSS4B based on the frequency-domain margin index of the MIMO system, which considered the critical gain constraint and optimized the characteristics while ensuring that the designed PSS4B provided the appropriate phase compensation. [8] showed a new method of nonlinear adaptive switching control to ensure the stability and convergence of the closed-loop switching system. [9] combined the recursive least square method with Vinnicombe distance to form a new iterative identification method, which could effectively suppress the low-frequency oscillation of the power system with wind power. [10] used a static synchronous compensator, a static synchronous series compensator and a rotor-side converter. To compensate DFIG reactive power, a method for coordinated design was proposed based on the network predictive control (NPC), which could improve the damping and compensate the time delay when sending wide-area signals. [11] proposed a unified controller (UPFC) to suppress subsynchronous harmonic vibration in the hybrid power system that connected to the infinite bus through a series of capacitor compensation lines. [12] used a new dual PI controller based on UPFC and optimized it with its improved GWO technology. From the system responses and characteristic values, it was observed that the dual PI controller was better than the traditional PI controller. [13] proposed an organized structure of a doubly fed induction generator wind farm with a power oscillation damper (POD) and an adjustable error-driven stabilizer to increase the response of the low-frequency oscillation in the charging energy system. [14] proposed a new sparse-promoted adaptive control method for online self-tuning of PSS parameters, which could make PSS achieve better damping oscillation performance and robustness to wind energy changes. In [15], an adaptive control method of fuzzy hierarchical sliding mode was proposed to verify the boundedness of all signals in the closed-loop system by means of Lyapunov stability theory. By developing a specific cost function related to SMS, the original control problem in [16] was equivalent to the problem of finding a series of optimal control strategies. [17] designed a switching state observer of neural networks (NNs) to estimate the unmeasured system state and solved the output constraint problem by introducing the potential barrier Lyapunov function. [18] proposed a new H∞ tracking performance index, which considered the case that the control coefficient in the controlled output variable was not zero and was more general than the previous performance index.

However, the problem of low-frequency oscillation in the power system solved by the above references can only work under a single operating condition and cannot face the switching control of disturbances from various aspects after the wind power is connected to the power system. The main contribution of this paper is to design a linear iterative identification of low-frequency oscillation controller and three kinds of nonlinear unknown increment controller suitable for different working conditions to suppress the low-frequency oscillation of the power system. A new kind of switching control strategy is designed to four kinds of controllers, which can achieve an ideal control effect under different conditions. The new controller of low-frequency oscillation in power system under multiple operating conditions with wind power grid-connected can improve current operating conditions when facing complex operating conditions. At the same time, the method of combined switching control with Vinnicombe distance can be used to switch controllers under different operating conditions by linear and nonlinear forms.

2. System Identification Model and Fundamental Theory

2.1. System Identification Model. This paper uses the following identification model of the power system for the closed-loop identification. The general nonlinear dynamic system with single-input and single-output can be written as

$$y(k+1) = f\left[y(k), y(k-1), \ldots, (k-n_s+1), u(k), u(k), \ldots, u(k-1), \ldots, u(k-m_s)\right], \tag{1}$$

where $u(k) \in R$, $y(k) \in R$, they are the input and output of the system at the moment. $f(\bullet) \in R$ is a continuously differentiable nonlinear function, and n_s and m_s are the orders of the system.

2.2. Fundamental Theory

2.2.1. Vinnicombe Distance. The Vinnicombe distance refers to the distance between two frequency responses, which is a measurement method of the distance between two transfer

functions and is expressed δ_v by symbols. The Vinnicombe distance between the two transfer functions G_1 and G_2 is expressed as

$$\delta_v(G_1, G_2) = \begin{cases} \max\limits_{\omega} \kappa\left(G_1\left(e^{j\omega}\right), G_2\left(e^{j\omega}\right)\right), & \text{satisfy formula (3),} \\ 1, & \text{not satisfy formula (3),} \end{cases} \tag{2}$$

$$\begin{cases} \left(1 + G_1^* \cdot G_2\right) \cdot e^{j\omega} \neq 0 \quad \forall\omega, \\ \omega\left(1 + G_1^* \cdot G_2\right) + \eta\left(G_2\right) - \tilde{\eta}\left(G_2\right) = 0, \end{cases} \tag{3}$$

$$\delta_v(G_1, G_2) = \begin{cases} \max\limits_{\omega} \kappa\left(G_1\left(e^{j\omega}\right), G_2\left(e^{j\omega}\right)\right) \text{satisfy formula (3),} \\ 1 \qquad\qquad\qquad\qquad \text{not satisfy formula (3),} \end{cases} \tag{4}$$

where $G_1^*(e^{j\omega}) = G_1(e^{-j\omega})$, $\eta(G_2)$ is the number of poles in the open right half plane of G_2. $\tilde{\eta}(G_1)$ is the number of poles in the closed right half plane of G_1; $\omega(x)$ is the winding number of the Nyquist curve of the transfer function x surrounding the dot counterclockwise. When x has poles on the imaginary axis, the Nyquist curve should avoid these poles. $\kappa(G1(e^{j\omega}), G2(e^{j\omega}))$ is the chordal distance of the projection point obtained by projecting G_1 and G_2 onto the unit Riemannian sphere.

2.2.2. Controller Design. Since the uncertain range of the controlled object increases after the wind power is connected to the power system, the traditional low-frequency oscillation controller cannot adapt to the control under various operating conditions.

Therefore, for different controlled objects, this paper adopts the switching control method to achieve the global dynamic characteristics of the objects with multiple models, and then establishes corresponding controllers based on multiple models to quickly respond to external needs through the scheduling strategy of different controllers. Meanwhile, two types of linear and nonlinear controllers are designed to obtain optimal control results of the controlled object by two different fitted models.

2.2.3. Adaptive Controller of the Linear System. As for the aspect of the linear system control, an iterative identification method is used to identify the system model. According to [9], the reduced power system model G is given, and the model G is calculated, then the initial controller model K is calculated according to the stability theory.

$$K = \frac{-0.2797z^2 + 0.1336z - 0.0606}{z^3 + 0.543z^2 - 0.5078z - 0.0098}. \tag{5}$$

The optimal power system model and the optimal damping controller model can be expressed as follows:

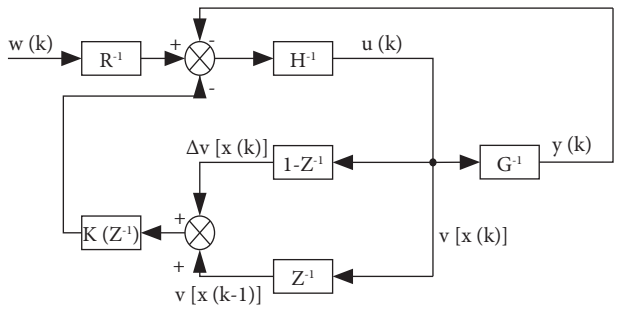

Figure 1: Switching control chart.

$$\begin{cases} G_{op} = \dfrac{1.0835z^2 + 2.9540z + 2.1717}{z^3 + 5.0142z^2 + 5.3237z + 5.067}, \\ K_{op} = \dfrac{-0.3137z^2 + 0.1403z - 0.0344}{z^3 + 0.6161z^2 - 0.5109z - 0.073}. \end{cases} \tag{6}$$

The controller design steps based on the iterative identification method are as follows:

Step 1: Through a given reduced-order model of the power system, an online iterative identification process is carried out using noise-like signals of low-frequency oscillation modes of the power system, and the iterative closed-loop identification is carried out based on the reduced-order model G by using the least squares method.

Step 2: According to the closed-loop stability condition of the power system $1 + GK = 0$, the initial linear controller model K is solved.

Step 3: According to the relevant Vinnicombe theory, the Vinnicombe distance $\delta_v(B_1, B_2)$ between the data B_1 obtained by the controller K and the theoretical data B_2 is solved by formula (2).

Step 4: According to the data obtained from Step 3, judge whether it satisfied$|\delta_v(B_1, B_2)| \leq 0.05$ (judge whether the error between the data obtained by the controller and the theoretical data is less than 0.05), and if conditions are met, the linear controller program ends. If the conditions are not met, return to Step 2 to continue calculating the calculation data of the controller.

2.2.4. Adaptive Controller of Nonlinear System. In terms of nonlinear controller, controllers under three different operating conditions are designed according to the increment of nonlinear terms. For the controlled object, a closed-loop nonlinear controller model is designed as shown in Figure 1. The nonlinear term $v[x(k)]$ in the output data is combined by forming an unknown estimated increment $\Delta v[x(k)]$ and the first row of linear data $v[x(k-1)]$.

2.2.5. Nonlinear Control Algorithm with Unknown Increment of Nonlinear Terms. According to formula (1), Taylor expansion at the origin can be obtained as

$$y(k+1) = -a_1 y(k) - \cdots - a_{n_s} y(k+1-n_s) + b_0 u(k) + \cdots b_{m_s} u(k-m_s) + v[x(k)]. \quad (7)$$

In which a_n and b_m are the first-order coefficients at the working place. $x(k)$ is a data vector which is defined as

$$x(k) = [y(k), \ldots y(k+1-n_s), u(k), \ldots, u(k-m_s)]^T. \quad (8)$$

$v[x(k)]$ is a smooth nonlinear function of the higher order, that is, it contains unmodeled dynamics. According to Figure 1, it can be seen that $v[x(k)]$ consists of the previous beating value $v[x(k-1)]$ and the estimated increment of the nonlinear term. $v[x(k)]$ consists of two parts, which can be expressed as

$$v[x(k)] = v[x(k-1)] + \Delta v[x(k)]. \quad (9)$$

Therefore, after adding the unit delay operator $z-1$, the system (7) can be further expressed as

$$A(z^{-1}) y(k+1) = B(z^{-1}) u(k) + v[x(k-1) + \Delta v[x(k)]. \quad (10)$$

The nonlinear controller (10) can be considered in three cases. If the unmodeled dynamic changes are not very intense, the estimated increment of the nonlinear terms at this time is small and negligible, so the controller can be designed as follows:

$$A(z^{-1}) y(k+1) = B(z^{-1}) u(k) + v[x(k-1)]. \quad (11)$$

If the unmodeled dynamic change is too intense, the unknown increment of the nonlinear term cannot fully compensate the loss compensation of the previous beating. The current beating of the nonlinear term and the square term of the nonlinear increment is used for the compensation design, so the controller can be designed as follows:

$$A(z^{-1}) y(k+1) = B(z^{-1}) u(k) + v[x(k-1)] + \Delta v[x(k)]^2. \quad (12)$$

2.2.6. Estimation Algorithm of Unknown Increment with Nonlinear Term. It is necessary to design the estimation algorithm and estimation identification equation for this increment because it is very important to use the estimation increment of the nonlinear term. According to equation (7), the parameter identification equation with the incremental estimation algorithm of the nonlinear term can be rewritten as

$$\hat{y}(k+1) = -a_1 y(k) - \cdots - a_{n_s} y(k+1-n_s) + b_0 u(k) + \cdots b_{m_s} u(k-m_s) + v[x(k-1)] + \Delta \hat{v}[x(k)]. \quad (13)$$

The unknown estimation algorithm and the nonlinear incremental estimation algorithm in [8] and [10] are adopted.

2.2.7. Switching Control. The linear controller of the iterative identification mentioned above and three kinds of nonlinear unknown incremental controllers are controlled by the following control strategies, thus forming a closed-loop structure of the control system. In this control strategy, the ideal result values of the output data are compared with output results of the above four controller models. The optimal performance index is introduced to screen out the above controllers, and the controllers are switched according to the tracking error value between the output values and the ideal values. Finally, a switching function is proposed as shown in Figure 2, and the related switching controller is performed according to its performance index. The switching function is as follows:

$$J_i(k) = \sum_{l=1}^{k} \frac{a_i(l)\left(e_i^2(l) - 4\Delta^2\right)}{2\left(1 + |w(l-1)|^2\right)} + \lambda \sum_{l=k-N+1}^{k} (1 - a_i(l)) e_i^2(l), \quad (14)$$

where $\sum_{l=1}^{k} a_i(l)(e_i^2(l) - 4\Delta^2)/2(1 + |w(l-1)|^2)$ is in order to distinguish the growth speed of different signals of the controlled system, and the robustness of the system is increased. ei(l) is the dead zone error. When $i=1$, the linear iterative model is used for the calculation. When $i=2$, the nonlinear controller of formula (10) is used to calculate the model. When $i=3$, the nonlinear controller of formula (11) is used to calculate the model. When $i=4$, the model is calculated by using the nonlinear controller of formula (12).

2.2.8. Overall Control Algorithm Steps. In the aspect of system control, an iterative identification is used to deal with the linear system, and nonlinear incremental compensation is used to deal with the nonlinear system, and then the system switching is carried out by switching the control system. The overall control flow chart is shown in Figure 3, and the overall design steps are as follows:

Step 1: Through the reduced-order model of the given power system and iterative identification initial controller C, the low-frequency oscillation mode by the noise-like signal of the power system is used for the online iterative identification processing.

Step 2: Classify the system according to online identification results and distinguish between linear systems and nonlinear systems.

Step 3: The data are transmitted to the linear system part and the nonlinear system part. For the nonlinear system part, the data are estimated with nonlinear unknown increment for the parameter identification, and the data are transmitted to the ignored unknown increment controller C_1, the controller C_2 with unknown

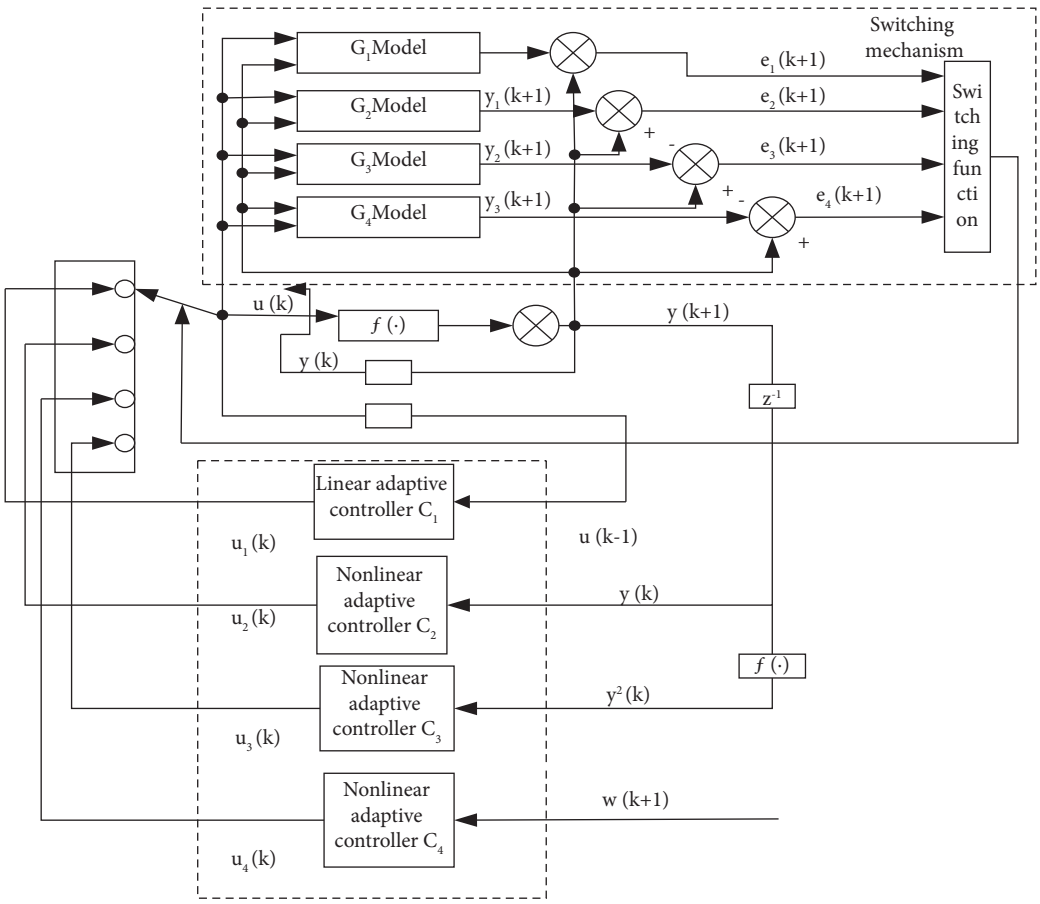

Figure 2: Overall switching schematic diagram.

increment, and the controller C_3 with unknown increment square term. For the linear system, the least square method is used to identify the system model G, and then the data are transmitted to the iterative identification optimization controller C_4 for calculation.

Step 4: Judge the distance between the results output by the four controllers and the ideal identification results by using the Vinnicombe distance theory. If the distance between the output of controller C_1 and the ideal output exceeds 0.05 (judging whether the error between the data obtained by the controller and the theoretical data are greater than 0.05), then return to Step 3 to reidentify and calculate the nonlinear part shown in Figure 3. The same rule is for controllers C_2 and C_3. If the distance between the output of controller C_4 and the ideal output exceeds 0.01, return to Step 3 to re-identify and calculate the linear part shown in Figure 3.

Step 5: The kinds of output data results of four controllers are transmitted to the switching function for calculation, and the optimal controller is screened out through the switching function and the controller position is switched to the system control.

Step 6: Use the optimal performance index J to judge the selected optimal controller, and judge whether the optimal performance index J of the adopted controller is the smallest among the optimal performance indexes of the four controllers (judging whether the adopted controller is the optimal controller for the system among the four controllers). If $J = \min[J_j]$, the controller ends. If not, go back to Step 5 and continue to calculate the control data for the switching function.

3. Simulation Verification

In the MATLAB simulation, the PMU data and IEEE 39 nodes of 10 machines are used as the basic data of the simulation verification in Figure 4, and the voltage data of Sub1 and the top 1600 beats of Ln1 are mainly used as the input data of this simulation.

Taking the PMU data system as an example, the input data model is simulated and verified, and 400×4 are selected from the PMU voltage data. They are used as the initial input data of the system. According to Step 1 of the algorithm in this paper, the reduced-order power system model is given

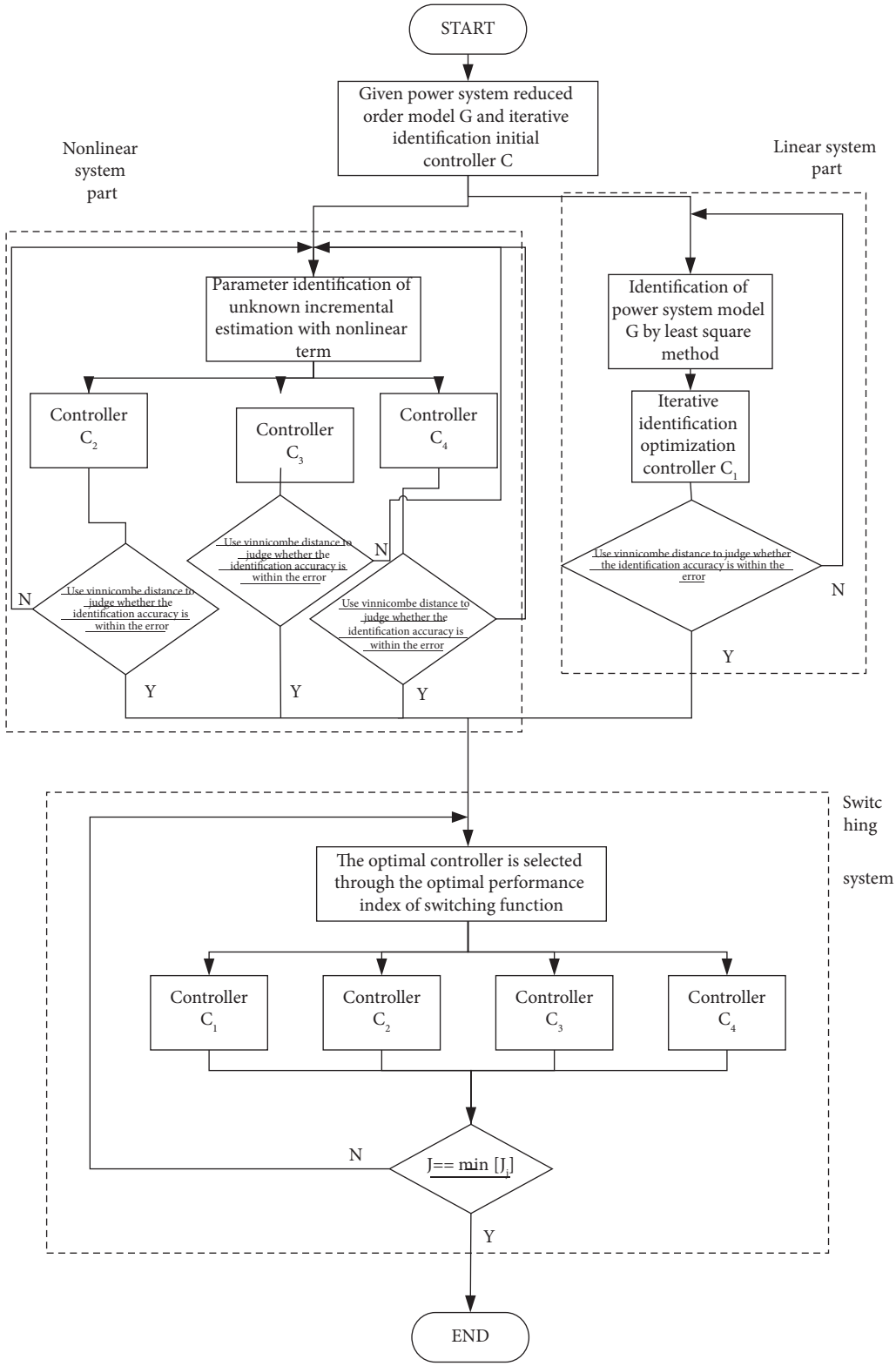

Figure 3: Overall control flow chart.

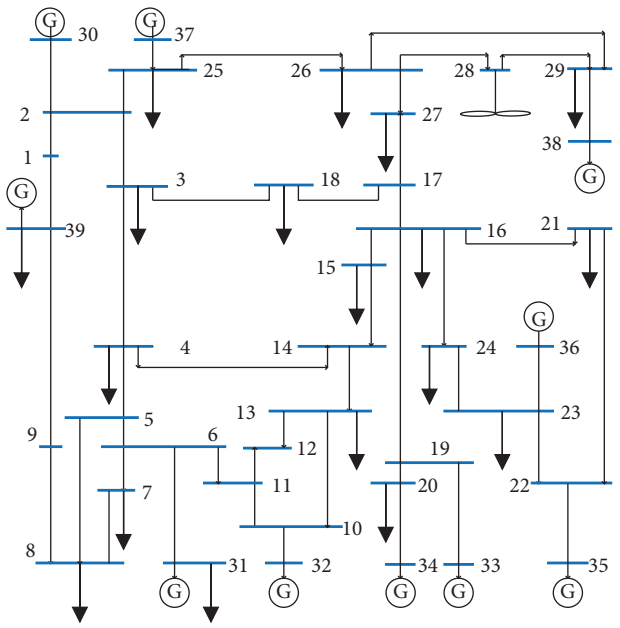

Figure 4: The New England 10 machine 39 node system.

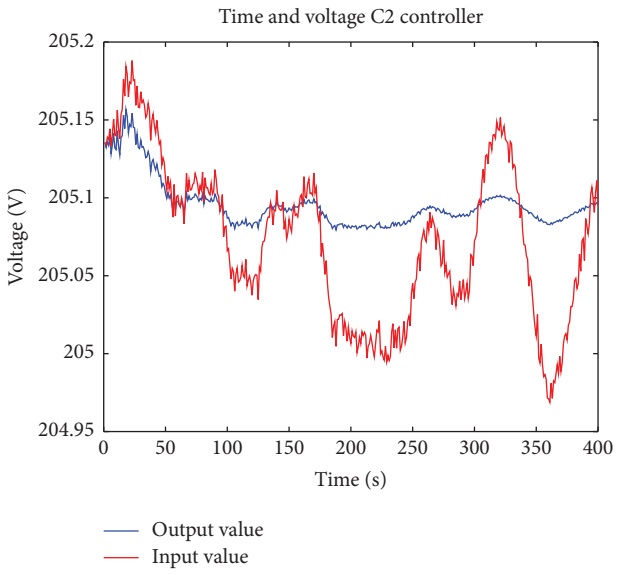

Figure 5: C_2 controller.

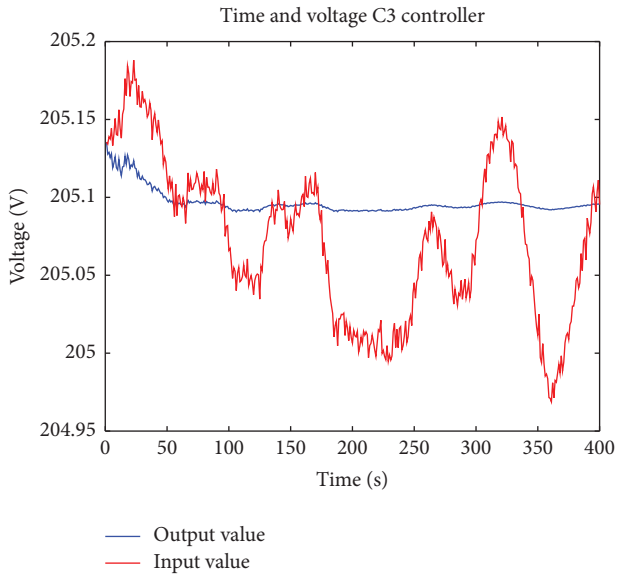

Figure 6: C_3 controller.

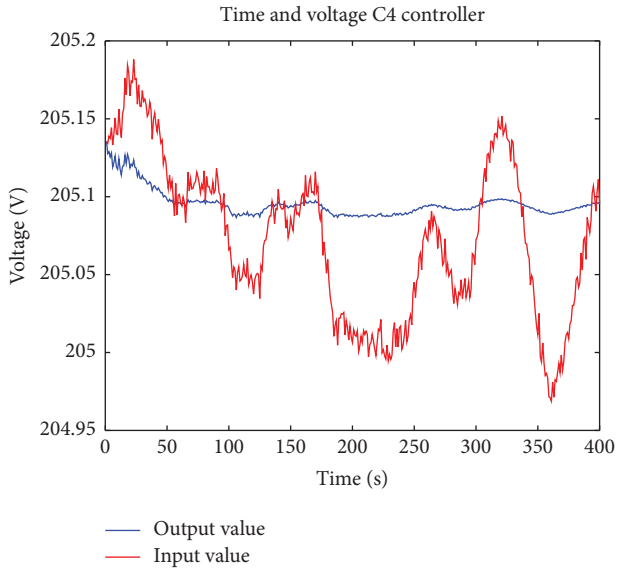

Figure 7: C_4 controller.

first, and then the iterative identification initial controller model is calculated according to the system stability theory. Pass the input data by Steps 3 and 4.

Among the switching functions, the selection of the constant λ in the switching control function has a certain impact on the smoothness of the performance of the switching function. In the simulation example, an interval from 1 to 1000 for the constant λ is selected and a step size is chosen as 10. Then, the optimal constant $\lambda'(\lambda' = 80)$ is selected from the interval according to the input PMU data to achieve better control performance.

When the controller is manually selected, the output data of the same group after passing through the C_2, C_3, and C_4 controllers are shown from Figures 5–7.

Figure 8 is the diagram of the switching control sequence, which clearly shows the selection and switching of four controllers by the switching function.

Figure 9 is an input and output data after controlling the smooth switching of the abovementioned linear iterative controller and the nonlinear unknown increment controller by the switching function of the present scheme.

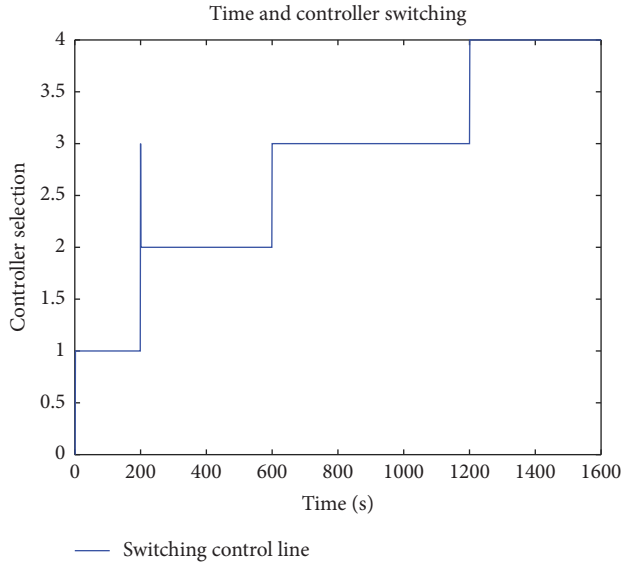

Figure 8: Switching control sequence.

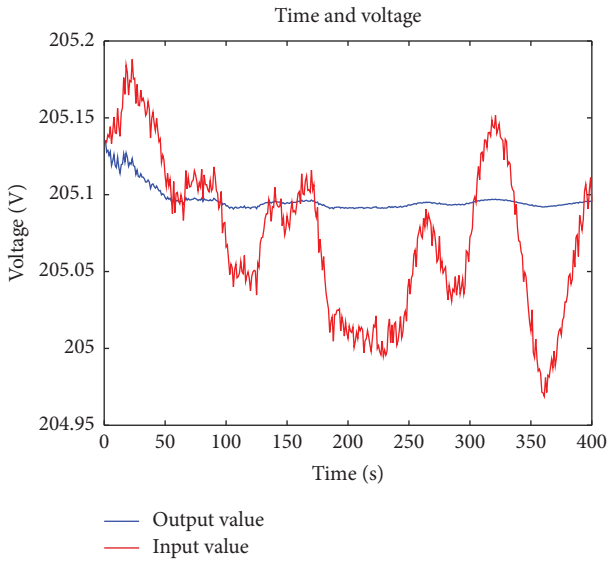

Figure 9: General controller.

Figure 10 shows the control effect comparison between this scheme and the traditional single PID controller. From Figure 10, it can be seen that this scheme has better control effect in the low-frequency oscillation control. The control effect of a single PID controller fluctuates in a large range, and this scheme can control the low-frequency oscillation of the power system in a short time and stabilize the results in a small range.

Through the simulation data, it can be seen that the front-end input PMU voltage data with low-frequency oscillation gradually tend to a stable state by the adjustment and control of the controller.

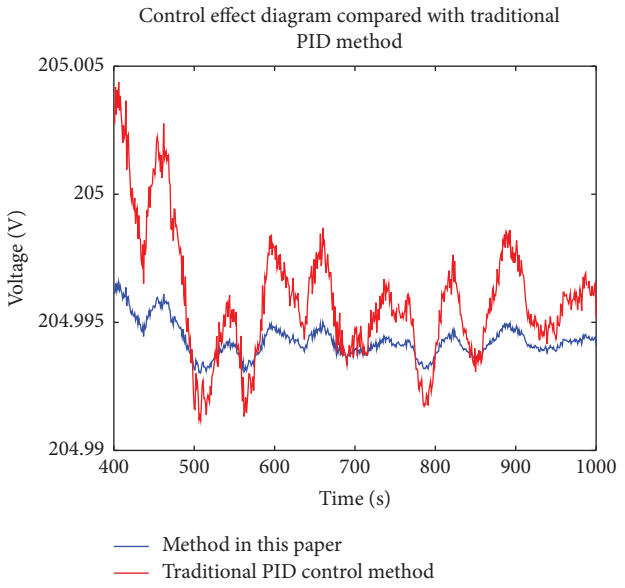

Figure 10: Control effect compared with the traditional PID method.

4. Conclusions

According to the current large number of wind power connected to the power system and PMU data processing, a new adaptive switching control algorithm combining linear and nonlinear is proposed for the discrete-time dynamic system. In terms of controller design, a class of linear iterative identification controllers and three types of nonlinear unknown incremental compensation controllers are designed according to the low-frequency oscillation of the actual power system. The compensation increment of the current beating is carried out by using the difference between the previous row of data of the nonlinear system and the current data. At the same time, the compensation increment is changed according to the actual power system, and it can better fit the real power system. Finally, the four controllers are coordinated and switched by using the optimal performance index through the switching function. According to the simulation data of the MATLAB system, the control algorithm has good stability and convergence. Therefore, the method proposed in this paper can realize the low-frequency oscillation control of wind power connected to the power system and can effectively suppress the low-frequency oscillation of the power system in the environment of wind power connected. In the future, we will continue to optimize the switching control algorithm based on four controllers of this scheme. At present, since the constant term of the switching control algorithm in this scheme is selected from 1 to 1000, the switching effect may not reach the optimal effect in a wide range of power system. Therefore, we will continue to optimize the switching control algorithm, so as to achieve the optimal effect of the controller switching.

Data Availability

No underlying data were collected or produced in this study.

Conflicts of Interest

The authors declare that there are no conflicts of interest regarding the publication of this paper.

Acknowledgments

The authors would like to thank Jingjing Wei, Jianqun Sun, and Yixiao Wu for their excellent technical supports and Professor Shanming Wang for critically reviewing the manuscript. The work of Miao Yu was supported by the State Key Laboratory of Pyramid Talent Training Project of Beijing University of Civil Engineering and Architecture (JDYC20200324); Graduate Education and Teaching Quality Improvement Project of Beijing University of Civil Engineering and Architecture (J2022007); BUCEA Post Graduate Innovation Project (PG2021090 and PG2022132); Security Control and Simulation for Power System and Large Power Generation Equipment (SKLD20M17); National Innovation and Entrepreneurship Training Program for College Students (202110016052, S202110016122, S202110016123, X202110016177, X202110016178, and X202110016179); Project of Beijing Association of Higher Education (YB2021131); Social Practice and Innovation and Entrepreneurship Curriculum Project of Beijing University of Civil Engineering and Architecture (SJSC1913); National Natural Science Foundation of China (51407201); Education, Teaching, and Scientific Research Project of China Construction Education Association (2021051).

References

[1] P. X. Liu, Y. B. Jia, and Y. H. Luo, "Research on low-frequency oscillation modes and factors of regional power grid with wind power based on EWT and improved Prony algorithm," *Electric Measurement and Instrument*, vol. 58, no. 5, pp. 1–9, 2020.

[2] Q. L. Li, W. Huang, L. Chen, C. Wu, R. H. Duan, and Y. Min, "Mechanism and damping analysis method of the power system stabilizer that affects frequency oscillation," *Power system automation*, vol. 44, no. 01, pp. 67–73, 2020.

[3] A. J. Zhang, D. D. Li, Q. B. Zhang, H. D. Xing, and P. Shi, "Impact analysis of wind power grid connection on low-frequency oscillation mode based on vector margin method," *Power system automation*, vol. 45, no. 2, pp. 122–129, 2021.

[4] Y. H. Nie, H. T. Xu, G. W. Cai, Q. F. Zhang, and D. Y. Yang, "Coordinated optimization strategy of wide-area damping controller with doubly-fed wind turbine system," *Power Automation Equipment*, vol. 40, no. 10, pp. 79–84, 2020.

[5] X. J. Pan, L. W. Zhang, W. C. Zhang, Y. P. Xu, H. Y. Bian, and X. J. Wang, "Multi-operation mode parameter coordination and optimization method of power system stabilizer based on Moth Fire Fighting optimization algorithm," *Power Grid Technology*, vol. 44, no. 8, pp. 3038–3046, 2020.

[6] Q. L. Li, C. Wu, L. Chen, R. H. Duan, W. Huang, and Y. Min, "Power System Stabilizer parameter optimization for suppressing frequency oscillation," *Power system automation*, vol. 44, no. 7, pp. 93–99, 2020.

[7] C. X. Jiang, P. Shi, W. Huang, Z. J. H. Zhou, and D. Q. Gan, "Considering the multi-frequency band power system stabilizer parameter setting method of multi-oscillation mode," *Power system automation*, vol. 44, no. 4, pp. 142–149, 2020.

[8] H. Niu, J. M. Tao, and Y. J. Zhang, "A new data-driven nonlinear adaptive switching control method," *Journal of Automation*, vol. 46, no. 11, pp. 2359–2366, 2020.

[9] M. Yu, W. P. Shang, Z. C. Yuan, and J. Y. Yi, "Damping control of wind power power system based on iterative identification method," *Power system automation*, vol. 41, no. 23, pp. 61–67, 2017.

[10] M. Darabian and A. Jalilvand, "Designing a wide area damping controller to coordinate FACTS devices in the presence of wind turbines with regard to time delay," *IET Renewable Power Generation*, vol. 12, no. 13, pp. 1523–1534, 2018.

[11] L. Wang, S. Y. Zeng, W. K. Feng et al., "Damping of subsynchronous resonance in a hybrid system with a steam-turbine generator and an offshore wind farm using a unified power-flow controller," *IEEE Transactions on Industry Applications*, vol. 57, no. 1, pp. 110–120, 2021.

[12] N. Nahak, S. R. Sahoo, and R. K. Mallick, "Design of dual optimal UPFC based PI controller to damp low frequency oscillation in power system," in *Proceedings of the 2018 Technologies For Smart-City Energy Security And Power (ICSESP)*, pp. 1–5, Bhubaneswar, India, March 2018.

[13] G. L. Fan, F. Yang, P. X. Guo, C. Xue, S. Gholami Farkoush, and J. Karimpoor Majd, "A new model of connected renewable resource with power system and damping of low frequency oscillations by a new coordinated stabilizer based on modified multi-objective optimization algorithm," *Sustainable Energy Technologies and Assessments*, vol. 47, pp. 101356–101417, 2021.

[14] G. Z. Zhang, W. H. Hu, D. Cao, Q. Huang, Z. Chen, and F. Blaabjerg, "A novel deep reinforcement learning enabled sparsity promoting adaptive control method to improve the stability of power systems with wind energy penetration," *Renewable Energy*, vol. 178, pp. 363–376, 2021.

[15] H. Y. Zhang, N. Xu, G. D. Zong, and A. F. Alkhateeb, "Adaptive fuzzy hierarchical sliding mode control of uncertain under-actuated switched nonlinear systems with actuator faults," *International Journal of Systems Science*, vol. 52, no. 8, pp. 1499–1514, 2021.

[16] H. Y. Zhang, H. Q. Wang, B. Niu, L. Zhang, and A. M. Ahmad, "Sliding-mode surface-based adaptive actor-critic optimal control for switched nonlinear systems with average dwell time," *Information Sciences*, vol. 580, pp. 756–774, 2021.

[17] Y. W. Zhao, H. Y. Zhang, Z. Y. Chen, H. Q. Wang, and X. D. Zhao, "Adaptive neural decentralised control for switched interconnected nonlinear systems with backlashlike hysteresis and output constraints," *International Journal of Systems Science*, vol. 53, no. 7, pp. 1545–1561, 2022.

[18] X. H. Chang, Y. W. Jing, X. Y. Gao, and X. P. Liu, "H-∞ tracking control design of T-S fuzzy system," *Control and Decision*, vol. 23, no. 3, pp. 329–332, 2008.